

Statespecific study of hydrogen desorption from Si(100)(2×1): Comparison of disilane and hydrogen adsorption

S. F. Shane, K. W. Kolasinski, and R. N. Zare

Citation: *J. Vac. Sci. Technol. A* 10, 2287 (1992); doi: 10.1116/1.577932

View online: <http://dx.doi.org/10.1116/1.577932>

View Table of Contents: <http://avspublications.org/resource/1/JVTAD6/v10/i4>

Published by the AVS: Science & Technology of Materials, Interfaces, and Processing

Related Articles

Cooperative photoinduced two-dimensional condensation in Langmuir films observed using nanosecond pump-probe Brewster angle microscopy
Biointerphases 5, FA105 (2010)

Adsorption mechanism of arg-gly-asp on rutile TiO₂ (110) surface in aqueous solution
J. Vac. Sci. Technol. B 27, 1548 (2009)

The direct injection of liquid droplets into low pressure plasmas
J. Vac. Sci. Technol. A 27, 342 (2009)

Experimental studies of the cap structure of single-walled carbon nanotubes
J. Vac. Sci. Technol. B 21, 868 (2003)

Outgassing of photoresist materials at extreme ultraviolet wavelengths
J. Vac. Sci. Technol. B 18, 3364 (2000)

Additional information on *J. Vac. Sci. Technol. A*

Journal Homepage: <http://avspublications.org/jvsta>

Journal Information: http://avspublications.org/jvsta/about/about_the_journal

Top downloads: http://avspublications.org/jvsta/top_20_most_downloaded

Information for Authors: http://avspublications.org/jvsta/authors/information_for_contributors

ADVERTISEMENT

Instruments for advanced science

Gas Analysis



- dynamic measurement of reaction gas streams
- catalysis and thermal analysis
- molecular beam studies
- dissolved species probes
- fermentation, environmental and ecological studies

Surface Science



- UHV TPD
- SIMS
- end point detection in ion beam etch
- elemental imaging - surface mapping

Plasma Diagnostics



- plasma source characterization
- etch and deposition process reaction kinetic studies
- analysis of neutral and radical species

Vacuum Analysis



- partial pressure measurement and control of process gases
- reactive sputter process control
- vacuum diagnostics
- vacuum coating process monitoring

contact Hiden Analytical for further details

HIDEN ANALYTICAL

info@hideninc.com
www.HidenAnalytical.com

CLICK to view our product catalogue 

State-specific study of hydrogen desorption from Si(100)-(2×1): Comparison of disilane and hydrogen adsorption

S. F. Shane, K. W. Kolasinski, and R. N. Zare
Department of Chemistry, Stanford University, Stanford, California 94305

(Received 1 October 1991; accepted 4 November 1991)

The desorption of hydrogen from the monohydride species on Si(100) has been studied state specifically using $(2 + 1)$ resonance-enhanced multiphoton ionization. The monohydride phase was prepared by dosing the surface with either disilane (Si_2H_6) or atomic hydrogen. Adsorption of disilane with subsequent desorption of H_2 leads to the growth of an epitaxial silicon film, based on evidence obtained with scanning electron microscopy and low energy electron diffraction. We report that the rovibrational-state distribution for hydrogen desorbed from Si(100) is the same after both disilane and atomic-H adsorption. Hydrogen desorbs with low average rotational energy but with a population in the $\nu = 1$ state enhanced by roughly 20 times over a thermal distribution at the temperature of the surface. The agreement between internal-state distributions for both adsorption schemes indicates that the desorption of hydrogen during epitaxial growth of Si after Si_2H_6 adsorption proceeds in the same manner as that for a hydrogen-prepared Si(100)-(2×1):H surface.

I. INTRODUCTION

Recently, the hydrogen-silicon system has received much attention. Many studies have focused on the structure of hydride-covered silicon surfaces,¹⁻⁵ the kinetics of desorption and diffusion of adsorbed hydrogen,⁶⁻¹⁴ and the role of these structures and processes in the chemical vapor deposition (CVD) of silicon.¹⁵⁻²⁰ The silicon-hydride species in most studies are typically prepared by one of two methods—either by adsorption of hydrogen in its atomic form or by adsorption of Si-containing precursors such as disilane, Si_2H_6 . Both atomic hydrogen and disilane are much more reactive toward a silicon surface than is molecular hydrogen, which has an extremely low sticking probability on Si.^{21,22} In this article, we use dynamical measurements to address the question of how similar on an atomic scale are the surfaces prepared in these two ways.

Several studies have shown that both hydrogen and disilane adsorption lead to the formation of monohydride, dihydride, and trihydride species on the Si(100)-(2×1) and the Si(111)-(7×7) surfaces.^{16,19,23,24} However, the presence of the higher hydrides is highly coverage and temperature dependent, with the higher hydrides being favored at lower temperatures and higher coverages. A saturation dose of disilane can lead to different relative coverages of the various hydride species compared to a saturation dose of atomic hydrogen at the same temperature. For example, at the surface temperature used in this study ($T_s \sim 400$ K), adsorption of disilane leads primarily to the formation of monohydride units, whereas adsorption of atomic hydrogen leads to a roughly 1:3 ratio of dihydride to monohydride species. This complex behavior is attributed to the instability of the higher hydrides in the presence of available dangling bonds.²⁴ In this article, we focus only on the monohydride species.

One major difference between adsorption of atomic hydrogen and adsorption of Si_2H_6 is the presence of new silicon adatoms on the Si(100) surface. We must ask what

role these deposited silicon atoms play in the details of hydrogen desorption. Specifically, how well do studies of systems prepared by H-atom adsorption represent a reasonable model of disilane CVD under those conditions where hydrogen desorption is rate limiting?

Using multiple internal reflection (MIR) infrared spectroscopy, Uram and Jansson²³ found that after disilane adsorption on Si(111)-(7×7) at 400 K, only a broad, featureless spectrum was apparent, an observation which they attributed to surface disorder resulting from the deposition of additional surface silicon atoms. Several experiments indicate, however, that by the time the surface nears the hydrogen desorption temperature (~ 800 K for the monohydride), the surface resembles that produced by hydrogen adsorption. The temperature programmed desorption (TPD) spectra^{19,25} obtained after disilane adsorption on both Si(100)-(2×1) and Si(111)-(7×7) are very similar to those observed for a surface saturated by hydrogen, i.e., they exhibit the same two peaks, β_1 and β_2 , at approximately the same peak temperatures.²⁶ Suda *et al.*,¹⁸ in their electron energy loss spectroscopy (EELS) and reflection high-energy electron diffraction (RHEED) studies of the dihydride phase produced by disilane adsorption on Si(100), conclude that desorption from a Si_2H_6 -saturated (1×1):2H surface follows essentially the same reaction path as that of the H-saturated dihydride surface. Boland²⁰ has found using scanning tunneling microscopy (STM) that although random adsorption of disilane on Si(100) at room temperature leads to a disordered surface, heating to 650 K causes the surface to rearrange into rows of Si dimers due to the decomposition of higher hydrides at this temperature. Thus, these experiments suggest that the surface structure may be similar at the temperature of hydrogen desorption independent of whether disilane or atomic hydrogen is dosed.

In this article, we present the results of state-specific studies of hydrogen desorption from Si(100) after adsorption of both disilane and atomic hydrogen. We report that

the rotational and vibrational distributions of the desorbed hydrogen are the same independent of the source of surface hydrogen. Thus we provide *dynamical* evidence that the mechanism of recombinative hydrogen desorption after adsorption of disilane is the same as that for a surface dosed with atomic hydrogen.

II. EXPERIMENTAL

The experimental technique has been described in detail elsewhere.²⁷ The experiments are performed in an ultra-high vacuum (UHV) chamber with a base pressure of approximately 4×10^{-10} torr. Surface order and cleanliness are monitored with low-energy electron diffraction (LEED) and Auger electron spectroscopy (AES). The crystal samples are cut from wafers of highly As-doped Si(100). The low resistivity of the crystals ($0.005 \Omega \text{ cm}$) facilitates direct resistive heating. The crystals are cleaned initially by annealing for 12–24 h at 900 K, followed by an anneal at 1200 K to remove the native oxide. This procedure leads to a well-ordered Si(100)-(2×1) surface, which generally has some residual carbon contamination. The surface cleanliness is maintained by passivating with an adsorbed hydrogen layer between experiments.

Attached to the UHV chamber is a source chamber containing a pulsed, skimmed, and collimated molecular beam, which is used to dose the surface with disilane. Using a stagnation pressure of ~ 30 Torr and a pulse width of 2 ms (run at 10 Hz), the surface is saturated within 30–60 s. Atomic hydrogen for the H-atom dosing is produced by a hot tungsten filament placed a few centimeters from the surface while backfilling the chamber with H_2 .

The internal-state distributions of molecular hydrogen are determined using (2 + 1) resonance-enhanced multiphoton ionization (REMPI) through the $E, F^1\Sigma_g^+$ state. This scheme requires ultraviolet radiation in the range of 200–215 nm to probe $v = 0$ and $v = 1$, and is generated by frequency mixing the output of a Nd:YAG-pumped dye laser. The resulting 1–2 mJ of light is directed into the chamber parallel to the crystal face, and is focused a few millimeters above the surface with a 350 mm lens. Hydrogen ions produced by REMPI are extracted into a time-of-flight (TOF) tube and detected with a two-stage microchannel plate chevron detector. Reduction of the ion signal (power normalized) to accurate hydrogen state populations has been established.²⁸

The state-specific experiments are performed in the following way. After dosing the surface to saturation with either disilane (at $T_s = 375$ K) or atomic hydrogen ($T_s = 425$ K), a TPD is performed. The laser is tuned to a frequency corresponding to REMPI from a particular $\text{H}_2(v, J)$ -level during the TPD. The crystal is then cooled slowly, and another TPD is performed. We continue this procedure for each rovibrational quantum state. Thus, in the case of disilane adsorption, Si is added one atomic layer at a time.

After disilane experiments are run on a crystal for several weeks, the LEED pattern begins to lose its sharpness, and the crystals are replaced. Some of these crystals were examined by scanning electron microscopy (SEM). The

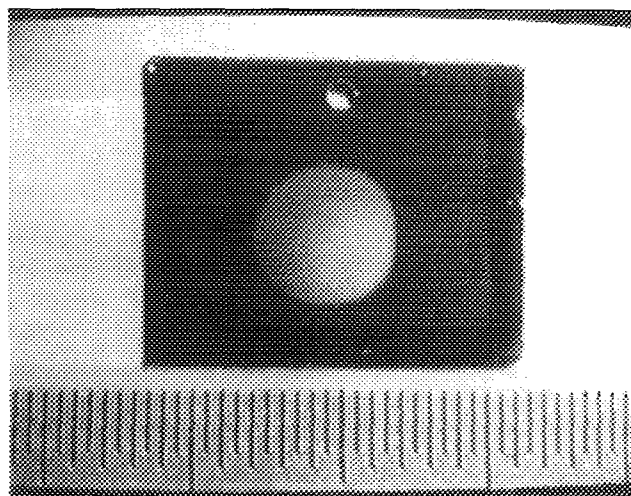


FIG. 1. Photograph of Si(100) crystal after chemical vapor deposition. The crystal was illuminated from the side. The 5 mm-diam circle in the center of the crystal is the region of silicon growth corresponding to the area of the disilane molecular beam. The hole at the top of the crystal was used to mount the thermocouple, and the bands at the sides of the crystal were caused by the crystal holder. The smallest interval on the scale corresponds to 0.5 mm.

samples were transferred from the vacuum chamber to a Phillips 505 microscope in air with no special precautions.

III. RESULTS

A. Silicon growth

A photograph of one of the silicon crystals used in the experiment is shown in Fig. 1. The hole at the top of the crystal was used for placement of the thermocouple that monitored the surface temperature during experiments. A spot of roughly 5 mm in diameter is visible in the center of the crystal. The appearance of this spot is caused by the growth of silicon from disilane, and its size corresponds closely to the diameter of our molecular beam of Si_2H_6 at the surface. The whiteness of the spot arises from the increase in scattered light where Si has been deposited. The LEED pattern still indicated a (100)-(2×1) pattern over this region of growth, and there was little variation in the LEED pattern across the crystal face.

A scanning electron micrograph of the surface within this 5 mm growth region is shown in Fig. 2. Micron-size rectangular shapes are evident on the surface, indicating that the growing film adopts the orientation of the underlying (100) surface. We are unable to determine from the SEM image whether these are projections or indentations. On this particular sample, the rectangular shapes make up roughly 10% of the surface area, though SEM images of other samples indicate that both the size and frequency varied with total silicon growth. Based on both the invariance of the LEED pattern during the growth of silicon and the observation of shapes of the correct symmetry by SEM, we conclude that the silicon film grows epitaxially on the Si(100)-(2×1) surface.

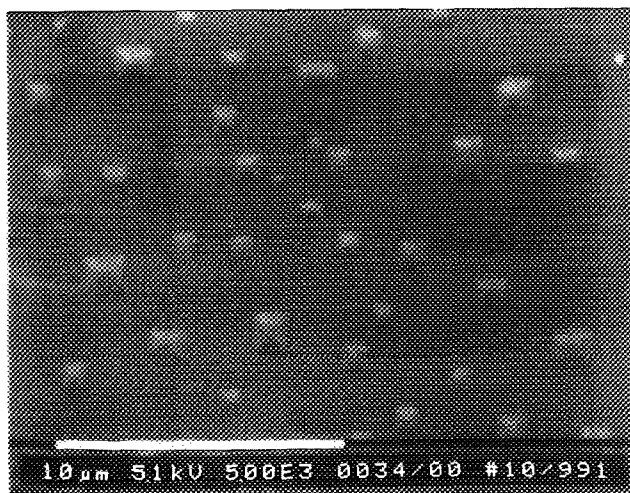


FIG. 2. Scanning electron micrograph of the Si(100) surface after chemical vapor deposition. The length of the white bar corresponds to 10 μm . Magnification was 5×10^3 and beam voltage was 5 kV.

B. Hydrogen desorption

A typical state-specific temperature programmed desorption for $\text{H}_2(v=0, J=1)$ is illustrated in Fig. 3. Desorption after saturation coverage of Si_2H_6 at $T_s = 375$ K is shown in Fig. 3(a), while Fig. 3(b) shows desorption after saturation exposure of atomic hydrogen at $T_s = 425$ K. Note that disilane adsorption leads to only a β_1 peak (the higher temperature peak related to desorption from the monohydride), while the β_2 desorption peak

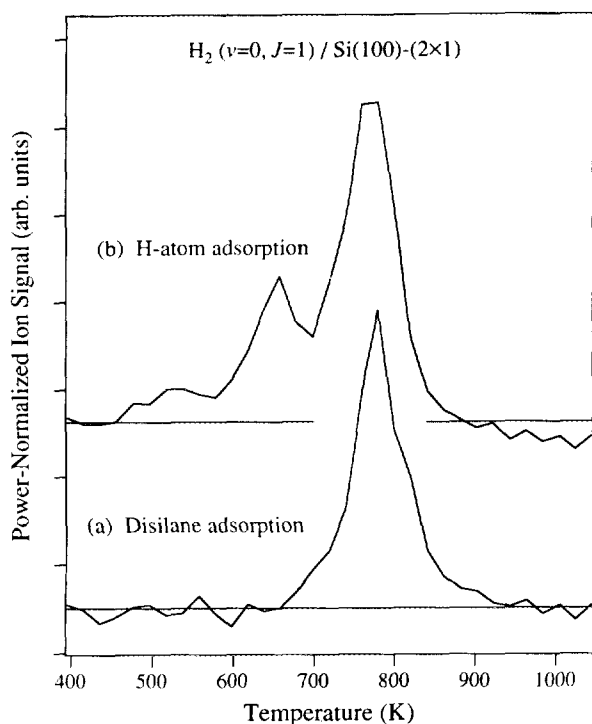


FIG. 3. Quantum-state-specific thermal desorption spectra for $\text{H}_2(v=0, J=1)$ desorbed from Si(100)-(2×1) after saturation dose of (a) disilane at $T_s = 375$ K and (b) atomic hydrogen at $T_s = 425$ K.

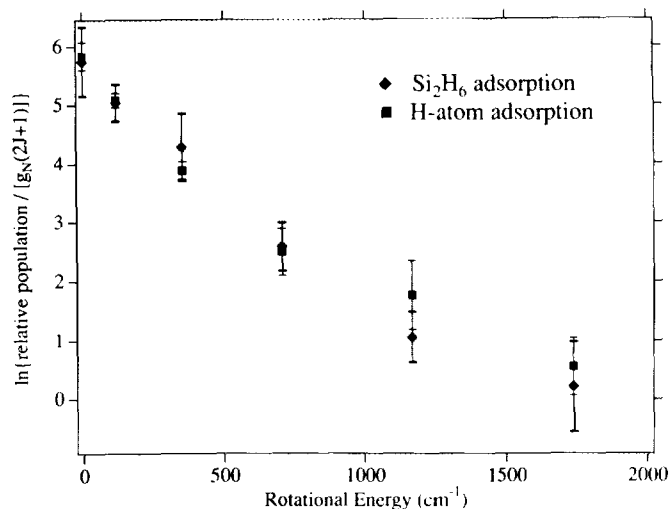


FIG. 4. Boltzmann plot of H_2 thermally desorbed from Si(100)-(2×1) in the ground vibrational state ($v=0$) after both disilane adsorption and atomic hydrogen adsorption.

(correlated with dihydride desorption) is clearly present after dosing with hydrogen.²⁵ Analysis of the β_2 desorption peak will be presented in another paper.²⁹ Integration of the β_1 peak for each rovibrational state, after correctly subtracting the background contribution¹³ and applying the proper correction factors,²⁸ leads to a population distribution. In Fig. 4, the rotational distribution for $\text{H}_2(v=0)$ is displayed in a Boltzmann plot, where the natural logarithm of the population divided by the rotational state degeneracy ($2J+1$) and the nuclear spin degeneracy (g_N) is plotted versus rotational energy.

The rotational distributions for hydrogen desorbed from Si(100) after Si_2H_6 and H-atom adsorption are clearly the same. The distribution is non-Boltzmann, i.e., it is not fit by a straight line, indicating that this is not a thermal distribution. The average rotational energy of these distributions, $\langle E_{\text{rot}} \rangle = \sum_j N_j E_j / \sum_j N_j$, is 345 ± 80 K for disilane dosing and 320 ± 70 K for H-atom dosing. The average rotational energies are the same within error bars, and significantly lower than the surface temperature at desorption, 800 K. Note that for a Boltzmann distribution at 800 K, $\langle E_{\text{rot}} \rangle = 783$ K \neq 800 K for H_2 , a nonclassical result caused by the large spacing of the hydrogen rotational levels. The hydrogen is clearly desorbing with an average rotational energy much lower than that expected for a Boltzmann distribution at the surface temperature.

In contrast, the vibrational distribution is superthermal. The population in $v=1$ for H_2 desorbing from Si(100) after disilane adsorption was found to be enhanced by a factor of about 25 over that of a thermal distribution at 800 K.²⁷ We report here that the vibrational enhancement is the same within error for hydrogen desorbing after adsorption of atomic H. Specifically, for both disilane and hydrogen adsorption, we measure $[N_{v=1}/N_{v=0}]_{\text{exp}} = 1.2\% \pm 0.5\%$, whereas for an 800 K thermal distribution, $[N_{v=1}/N_{v=0}]_{\text{Boltz}} = 0.05\%$. A model explaining the observed rovibrational distribution has been discussed in pre-

vious work.^{13,27} Briefly, we propose that desorption occurs through a symmetrically constrained transition state following pairing of adsorbed hydrogen, $H_{(a)}$, on Si dimers. This transition state is characterized by an H-H separation larger than that of the free H_2 molecule, resulting in product H_2 that is vibrationally excited but rotationally cold.²⁷

IV. DISCUSSION AND CONCLUSIONS

We observe that both the rotational- and vibrational-state distributions for H_2 desorbing from Si(100)-(2×1) are the same *whether the surface is dosed with disilane or by H atoms*. In the former case, the adsorption of disilane is clearly leading to the epitaxial growth of Si(100), as evident by the SEM and LEED results. However, the presence of deposited Si atoms does not appear to affect the rovibrational distribution of the desorbing H_2 .

Both rotational- and vibrational-state distributions might be expected to be sensitive to the dynamics of desorption and the transition state geometry and, therefore, to the structure of the surface. Previous studies of recombinative desorption from metal surfaces have suggested, however, that the vibrational distributions are much more sensitive to changes in surface structure and electronic properties of the surface than are the rotational distributions.³⁰⁻³² Studies of recombinative desorption of hydrogen on Cu have shown that the amount of vibrational excitation differs by a factor of two between the (110) and the (111) surfaces, while the rotational distributions are unchanged.³³ Studies of the recombinative desorption of H_2 from Cu,³⁰ H_2 from Pd,³¹ and N_2 from Fe (Ref. 32) have shown that modification of the surface electronic structure by coadsorption of sulfur dramatically affects the vibrational distribution.

Because we believe that the product internal-state distribution is a sensitive probe of the transition state, we conclude from our measurements of H_2 from Si(100)-(2×1) that the transition state geometries for recombinative desorption must be the same whether the surface is dosed with disilane or with atomic hydrogen. Note that we neglect the possibility of rotational-state-changing events occurring after molecular formation, based upon the results of isotopic studies.¹³ It appears, then, that the introduction of new Si atoms from disilane does not affect the mechanism of recombinative desorption. There are two possible interpretations of this result: (1) at 800 K, the Si adatoms have been incorporated into the lattice, yielding a surface that resembles that of the H-dosed Si(100)-(2×1) surface, or (2) desorption takes place at some local site that is independent of longer-range surface order.

Certainly, the STM²⁰ and TPD^{19,25} studies support the idea that the surface is reconstructed, at least partially, by 800 K. Boland observed that at 650 K, the dimer pairs, which are characteristic of the (100)-(2×1) reconstruction, could be found on the Si surface after adsorption of disilane.²⁰

However, it is not clear that the internal-state distribution of H_2 would be sensitive to *long-range* surface order. Because of the localized nature of bonding on the Si surface, the desorption mechanism probably involves very few

silicon atoms. Preliminary data from recent studies on the (111) surface³⁴ may lend some support to a local-site model. It is possible, then, that the surface might be disordered after adsorption of disilane, e.g., from Si adatoms that are not yet incorporated into the lattice, but that this disorder is not reflected in the internal-state distributions.

We have previously proposed that desorption occurs across a Si dimer pair. Conceivably, if desorption was entirely confined to the dimer pair, even an isolated dimer could yield a similar rovibrational distribution. The recombinative desorption mechanism would be insensitive to the ordering of the dimers with respect to one another. Desorption might even be localized to only one of the silicon atoms which make up a dimer pair. This could occur by a H-atom shift across the dimer followed by a three-center transition state for desorption.

We also cannot rule out the possibility that the local site from which H_2 desorbs is not in fact a Si dimer, but some defect site. Recent STM studies indicate that even on carefully prepared silicon surfaces, the defect density is quite large.^{35,36} It is useful to recall that dissociative adsorption of H_2 on Si(100)-(2×1) is an extremely low probability process. Thus, when H_2 does stick, it might be only at very specific sites on the surface that have a preferred geometry for H_2 adsorption. Using detailed balance, it would be these same minority sites from which H_2 desorbs. An appealing choice of adsorption site might be a Si atom with two dangling bonds. Again, a three-center transition state might be involved.

In either case, it is clear that the desorption dynamics *are the same whether disilane or atomic hydrogen is the source of surface silicon hydrides*. That is, the rovibrational distributions indicate that the same mechanism for recombinative desorption is active on both the hydrogen- and disilane-dosed surfaces, though further experiments are necessary to determine the specific desorption site. We conclude that H-atom adsorption/ H_2 desorption studies provide a reasonable model for hydrogen desorption under conditions of chemical vapor deposition using disilane.

ACKNOWLEDGMENTS

The authors would like to thank M. P. Hall for providing his expertise in the SEM studies and S. J. Clemett for taking the photograph of the surface. S. F. S. acknowledges support from a National Science Foundation Graduate Fellowship, and K.W.K. acknowledges the Procter & Gamble Foundation and Phi Beta Kappa of Northern California for fellowships. Funding was provided by the Office of Naval Research under Grant No. N00014-91-J1023.

¹Y. J. Chabal, Surf. Sci. **168**, 594 (1986); Y. J. Chabal and K. Raghavachari, Phys. Rev. Lett. **53**, 282 (1984); Y. J. Chabal, G. S. Higashi, K. Raghavachari, and V. A. Burrows, J. Vac. Sci. Technol. A **7**, 2104 (1989).

²J. J. Boland, Surf. Sci. **244**, 1 (1991); Science (in press).

³U. Jansson and K. Uram, J. Chem. Phys. **91**, 7978 (1989).

⁴S. Ciraci, R. Butz, E. M. Oellig, and H. Wagner, Phys. Rev. B **30**, 711 (1984).

⁵B. I. Craig and P. V. Smith, Surf. Sci. **226**, L55 (1990).

⁶G. Schulze and M. Henzler, Surf. Sci. **124**, 336 (1983).

- ⁷H. Froitzheim, U. Köhler, and H. Lammering, *Surf. Sci.* **149**, 537 (1985).
- ⁸B. G. Koehler, C. H. Mak, D. A. Arthur, P. A. Coon, and S. M. George, *J. Chem. Phys.* **89**, 1709 (1988).
- ⁹P. Gupta, V. L. Colvin, and S. M. George, *Phys. Rev. B* **37**, 8234 (1988).
- ¹⁰K. Sinniah, M. G. Sherman, L. B. Lewis, W. H. Weinberg, J. T. Yates, Jr., and K. C. Janda, *J. Chem. Phys.* **92**, 5700 (1990).
- ¹¹M. L. Wise, B. G. Koehler, P. Gupta, P. A. Coon, and S. M. George, *Surf. Sci.* **258**, 166 (1991).
- ¹²J. J. Boland, *Phys. Rev. Lett.* **67**, 1539 (1991).
- ¹³K. W. Kolasinski, S. F. Shane, and R. N. Zare, *J. Chem. Phys.* **95**, 5482 (1991).
- ¹⁴G. A. Reider, U. Hofer, and T. F. Heinz, *Phys. Rev. Lett.* **66**, 1994 (1991).
- ¹⁵See, for example, J. M. Jasinski, B. S. Meyerson, and B. A. Scott, *Annu. Rev. Phys. Chem.* **38**, 109 (1987); J. M. Jasinski and S. M. George, *Acc. Chem. Res.* **24**, 9 (1991), and references therein.
- ¹⁶C. M. Greenlief, S. M. Gates, and P. A. Holbert, *J. Vac. Sci. Technol. A* **7**, 1845 (1989).
- ¹⁷S. M. Gates, S. K. Kulkarni, and H. H. Sawin, *Proc. Electrochem. Soc. (Proc. Int. Symp. Process Phys. Model. Semicond. Technol., 2nd, 1990)*, p. 121.
- ¹⁸Y. Suda, D. Lubben, T. Motooka, and J. E. Greene, *J. Vac. Sci. Technol. B* **8**, 61 (1990).
- ¹⁹F. Bozso and P. Avouris, *Phys. Rev. B* **38**, 3943 (1988).
- ²⁰J. J. Boland, *Phys. Rev. B* **44**, 1383 (1991).
- ²¹J. T. Law, *J. Phys. Chem.* **30**, 1568 (1959).
- ²²W. Ho (private communication).
- ²³K. J. Uram and U. Jansson, *J. Vac. Sci. Technol. B* **7**, 1176 (1989).
- ²⁴R. Imbihl, J. E. Demuth, S. M. Gates, and B. A. Scott, *Phys. Rev. B* **39**, 5222 (1989).
- ²⁵S. M. Gates, *Surf. Sci.* **195**, 307 (1988).
- ²⁶We note that Bozso and Avouris also observe a broad H₂ desorption band below 450 K after adsorption of disilane at 100 K (Ref. 19).
- ²⁷K. W. Kolasinski, S. F. Shane, and R. N. Zare, *J. Chem. Phys.* (in press).
- ²⁸K.-D. Rinnen, M. A. Buntine, D. A. V. Kliner, R. N. Zare, and W. M. Huo, *J. Chem. Phys.* **95**, 214 (1991).
- ²⁹S. F. Shane, K. W. Kolasinski, and R. N. Zare (to be published).
- ³⁰G. D. Kubiak, G. O. Sitz, and R. N. Zare, *J. Vac. Sci. Technol. A* **3**, 1649 (1985).
- ³¹L. Schroter, R. David, and H. Zacharias, *Surf. Sci.* (in press).
- ³²R. P. Thorman and S. L. Bernasek, *J. Chem. Phys.* **74**, 6498 (1981).
- ³³G. D. Kubiak, G. O. Sitz, and R. N. Zare, *J. Chem. Phys.* **83**, 2538 (1985).
- ³⁴S. F. Shane, K. W. Kolasinski, and R. N. Zare (to be published).
- ³⁵R. M. Tromp, R. J. Hamers, and J. E. Demuth, *Phys. Rev. Lett.* **55**, 1303 (1985).
- ³⁶R. Wolkow (private communication).